Structure of concentrated nanoemulsions

S. Graves, K. Meleson, and J. Wilking
Department of Chemistry and Biochemistry, University of California-Los Angeles, Los Angeles, California 90095

M. Y. Lin
Center for Neutron Research, National Institute of Standards and Technology, Gaithersburg, Maryland 20899

T. G. Mason[a)]
Department of Chemistry and Biochemistry, University of California-Los Angeles, Los Angeles, California 90095 and Department of Physics and Astronomy, University of California-Los Angeles, Los Angeles, California 90095

(Received 11 October 2004; accepted 12 January 2005; published online 1 April 2005)

We use extreme shear to create a dispersion of nanoscale droplets of silicone oil in an immiscible water phase containing an anionic surfactant sodium dodecylsulfate. Using centrifugal size fractionation, we obtain nanoemulsions having a well-defined average radius of $a=75$ nm. We measure the structure of concentrated nanoemulsions over a wide range of volume fractions, $0<\phi<0.6$, using small angle neutron scattering, and we determine the structure factor $S(q)$ of disordered glassy dispersions of uniform deformable droplets interacting through screened surface charge repulsions. Although the low-q behavior of $S(q,\phi)$ resembles that predicted for hard spheres, the height of the primary peak does not. Instead, it exhibits a maximum as ϕ is increased. This difference cannot be explained solely by the droplet size polydispersity and is likely related to the deformability of the droplets that have been locked into a glassy structure. © *2005 American Institute of Physics*. [DOI: 10.1063/1.1874952]

I. INTRODUCTION

By contrast to equilibrium lyotropic liquid crystalline phases called "microemulsions"[1] which spontaneously form when the addition of surfactant effectively causes the surface tension to vanish,[2] "nanoemulsions" are metastable dispersions of submicron droplets that have a significant surface tension, which form only when extreme shear is applied to fragment droplets strongly, and are kinetically inhibited against recombining by repulsive interfacial stabilization due to the surfactant. Nanoemulsions represent the extremely small limit of emulsions[3] of submicron droplets known as "miniemulsions."[4–6] Although nanoemulsions have extreme Laplace pressures, of order 10–100 atm, the droplets can remain stable against Ostwald ripening[1,7] if the liquid inside has very low solubility in the continuous phase outside the droplets. The strong Brownian motion of the tiny droplets in nanoemulsions makes them ideal for products in which gravitational creaming must be prevented to ensure a long shelf life.

Although many investigations of the structure of hard particles have been made,[8] the study of the bulk structure of disordered deformable nanodroplets as a function of their volume fraction, ϕ, has not been extensively investigated and is fundamentally interesting. For nondeformable particles, the nature of the jamming point is known to depend on the shape of the particles, their interactions, and the driving forces present as the particles are concentrated to higher ϕ.[9,10] Nanoemulsions represent a promising system that will facilitate systematic studies of the structure of deformable particles since, in principle, the dispersed phase can be continuously controlled from zero to nearly unity through an applied osmotic pressure.[11] At dilute ϕ, the droplets are spherical, whereas at high ϕ, the surfaces of the droplets are strongly repelled by the surfaces of neighboring droplets. This can cause the droplets to deform and become nonspherical, yielding a biliquid nanofoam. An appropriate surfactant can strongly inhibit the droplets from recombining through interfacial coalescence, making nanoemulsions long-lived metastable liquid dispersions that have structures determined by the history of applied shear and osmotic pressure. By contrast, the structure of the dispersed phase in microemulsions is typically subject to morphogical changes[12] (e.g., from spherical droplet to a sponge structure or lamellar phase) when the volume fraction of the dispersed phase is changed appreciably. Such phase changes preclude investigations of microemulsions comprised spherical droplets over a wide range of droplet volume fractions.

Studies of disordered dispersions of solid particles[8,13–19] and of the liquid structures in foams[10,20–26] have provided a better understanding of the fundamental structure of disordered soft materials. These studies can be linked to the structure of emulsions because emulsion droplets are spherical for ϕ below the jamming limit, and can have interfacial structures like foams for ϕ above the jamming limit. Due to the strong Brownian motion of the nanoscale droplets, nanoemulsions do not cream or drain in the manner typically

[a)]Author to whom correspondence should be addressed.

observed for microscale and larger foams and emulsions. However, neither transmission nor scanning electron microscopy are well suited for examining liquid phases *in situ*, and cryofracture electron microscopy could potentially alter the morphology of the continuous phase structure in aqueous-based emulsions. Since microscopy methods for studying nanoscale emulsions have limitations, scattering methods provide a better method for obtaining the average structure of nanoemulsions in reciprocal space over a wide range of environmental conditions. Small angle neutron scattering (SANS) is a good candidate for obtaining the bulk structure of nanoemulsions, since the neutron wavelengths are suitable for probing nanoscale structures. Moreover, the scattering contrast in SANS can be controlled through deuteration of the components. Although wide-angle static light scattering of index-matched uniform microscale emulsions has been used to determine structure factors at a few concentrated volume fractions,[21,22] a clear systematic experimental investigation of the structure factor as a function of ϕ has not been made.

Through repeated ultracentrifugal fractionation of a polydisperse nanoemulsion, we obtain concentrated disordered nanoemulsions having a uniform size. We show that neutron scattering is an excellent probe of the structure of disordered nanoemulsions over a wide range of ϕ, even without enhancing the scattering contrast through selective deuteration. We measure the scattering intensity $I(q,\phi)$ of disordered nanoemulsions over a wide range of droplet volume fractions using SANS. From this, we show how the peak in the structure factor of concentrated nanoemulsions departs from predictions for disordered nondeformable spheres near and above the jamming point.

II. EXPERIMENT

We prepare oil-in-water nanoemulsions using the following procedure. Microscale droplets of silicone oil (polydimethylsiloxane) having a viscosity $\eta_d = 10$ cP are dispersed in H_2O at $\phi = 0.5$ and a high surfactant concentration of sodium dodecylsulfate (SDS), $C_{SDS} = 50$ mM, using a crude blender. The nanodroplets are formed by introducing this "premixed" microscale emulsion into an impinging jet device which periodically drives two pressurized streams of the premixed emulsion together to create violent extensional shear mixing and cavitation.[27] The resulting emulsion contains extremely small droplets, yet the droplet size distribution is not uniform. Premixing the emulsion helps to reduce the variability in the size distribution by keeping the volume fraction of droplets, and hence viscosity, in the jets relatively constant, yet it does not completely eliminate the compositional variation and thus variation in size. Due to the high surfactant concentration, these droplets do not coalesce or fuse back together. From this emulsification procedure, we obtain several hundred milliliters of a broad distribution of submicron oil droplets at a high concentration.

The classic method for separating polydisperse emulsions into several different monodisperse emulsions relies upon a micellar depletion attraction to induce size-dependent aggregation of larger droplets.[28] The flocs of larger droplets rapidly cream due to the density difference of the oil and the water. By separating the cream containing the larger droplets from the liquid containing the smaller droplets below and by repeating the procedure with a different micelle concentration, it is possible to fractionate the size distribution of the polydisperse emulsion. However, for this method to work effectively at reasonably small SDS concentrations, the droplet must be much larger than the size of the micelle (e.g., 2 nm for SDS). By contrast to microscale droplets, which are about a thousand times larger than the micelles, nanoemulsion droplets are less than 50 times larger. We have tried using depletion fractionation to separate nanoemulsions, but we cannot induce efficient flocculation even at very large micelle concentrations corresponding to $C_{SDS} = 100$ mM.

As an alternative to depletion fractionation, we make the size distribution of the nanoemulsion more uniform by employing a centrifugal size separation method based on the difference in creaming velocities of differently sized droplets.[29] First, the raw polydisperse emulsion is diluted with deionized water to $\phi = 0.2$, and this emulsion is introduced into a set of polycarbonate centrifuge tubes for use with a swinging bucket ultracentrifuge. These emulsions are spun at 18 000 rpm for 3 h at room temperature. This effectively applies an osmotic pressure to the emulsion, thereby concentrating all the droplets into a highly elastic plug at the top of the centrifuge tube, since the density of the silicone oil is less than that of water. Each plug has a gradient in both concentration of droplets and the size of the droplets; larger droplets at a higher volume fraction are generally at the top of the plug and smaller droplets at a lower volume fraction are generally at the bottom of the plug. The plugs are extracted from the tubes and split into different sections systematically; similar sections from different plugs are kept together. This effectively splits the droplet size distribution in each fractionation step. We repeat this process twice to obtain a uniform nanoemulsion for use in the neutron scattering studies. The last centrifugation step also serves to concentrate the nanoemulsion to high ϕ. To eliminate volume fraction gradients within the plug sections, the stock emulsion at high ϕ is allowed to equilibrate one week before measurements are performed.

SANS measurements have been carried out at room temperature using the NG-7 30 m beam line at NIST's Center for Neutron Research. The wavelength of the neutron beam is fixed at $\lambda = 8.1$ Å, and emulsions are loaded into quartz cells having a path length of 1.0 mm. Transmission measurements confirm that we are in the single scattering regime for all samples measured. Two different sample-detector distances are used to obtain intensities at low and high q. Collection times are typically about 1 h to obtain good statistics at low q. To control ϕ, we dilute the concentrated nanoemulsion with an aqueous solution of 10 mM SDS, stir with a small spatula, and allow the emulsions to equilibrate for at least 1 day. We then load the quartz cell and measure the scattered neutron intensity I as a function of the wave number q. The contribution of SDS to the scattering intensities that we observe is negligible. From these measurements, we obtain the structure factor $S(q,\phi)$ of disordered nanoemulsions from $0.01 \leqslant \phi < 0.6$.

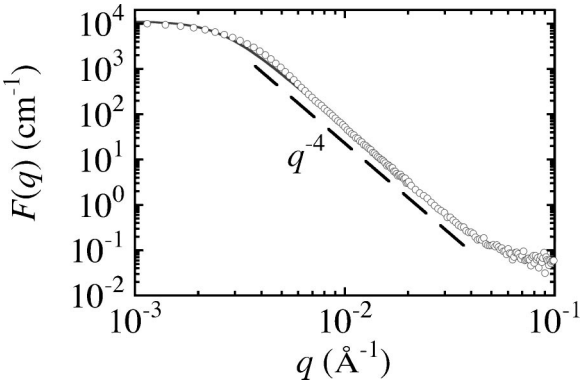

FIG. 1. Form factor $F(q)$ of a nanoemulsion diluted with D_2O at $\phi = 0.004$ measured using SANS. The solid line (almost indistinguishable from the data) is a fit to $F(q) = I_{inc} + I_0/[1+(q\xi)^4]$, and the dashed line represents a q^{-4} power law behavior beyond the knee. The average droplet radius obtained from $F(q)$ is $a = 75 \pm 10$ nm.

Because we will be dividing $I(q,\phi)$ by the measured form factor $F(q)$ in order to obtain $S(q,\phi)$, we need an excellent measurement of $F(q) = I(q, \phi \to 0)$ that has very little noise. In order to improve the measurement statistics of the form factor, we enhance the scattering contrast without introducing multiple scattering by diluting the concentrated emulsion with D_2O to $\phi = 0.004$, where the effects of the structure factor can be neglected.

III. RESULTS

The measured form factor $F(q)$ is shown in Fig. 1. We observe a plateau at low q and a decrease at larger q that varies as q^{-4} (dashed line) down to the constant incoherent scattering background. The shape of this form factor is characteristic of spheres having a unimodal distribution with an average radius of $a = 75 \pm 10$ nm and a polydispersity of about 25% that suppresses the sharp minima expected for highly monodisperse spheres. The data can be fit using the following equation: $F(q) = I_{inc} + I_0/[1+(q\xi)^4]$, where the incoherent scattering intensity is $I_{inc} = 0.05 \pm 0.01$ cm^{-1}, the low-q plateau intensity is $I_0 = 1.1 \pm 0.2 \times 10^4$ cm^{-1}, and the characteristic length is $\xi = 38 \pm 5$ nm (solid line). The average hydrodynamic radius a_h of the droplets was also measured using dynamic light scattering from a dilute solution of nanodroplets in H_2O. We find $a_h = 74 \pm 8$ nm, and, within the error, this matches the value obtained from the SANS form factor.

The measured scattering intensities $I(q,\phi)$ beyond the extremely dilute limit for dilute and concentrated nanoemulsions are shown in Figs. 2(a) and 2(b), respectively. In Fig. 2(a), as ϕ is raised, there is an increase in the plateau intensity at low q. However, for even larger ϕ, as shown in Fig. 2(b) the height of the low-q plateau decreases, and a peak in the scattering intensity develops at q values corresponding to the interdroplet separation. The q value associated with this peak moves to higher q as ϕ is increased.

IV. ANALYSIS

We divide $I(q,\phi)$ by $F(q)$ to obtain the structure factor $S(q,\phi)$ of the nanoemulsion, as shown in Fig. 3. At each ϕ, we ensure that the structure factor approaches unity at large

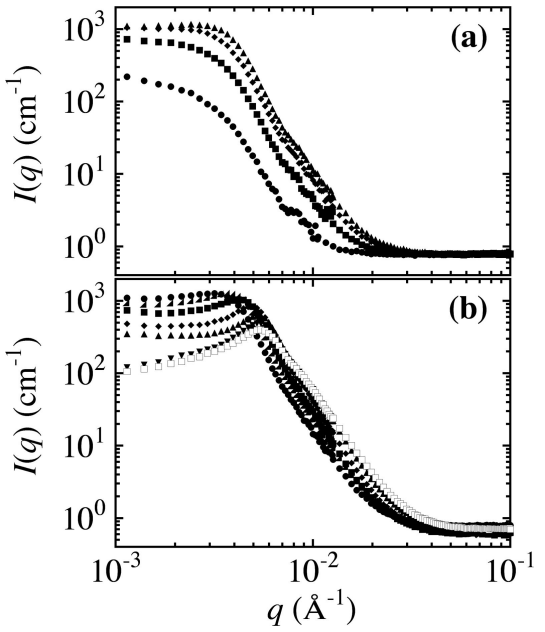

FIG. 2. SANS intensity $I(q)$ of semidilute nanoemulsions in H_2O for the following droplet volume fractions: (a) $\phi = 0.008$ (●), 0.039 (■), 0.079 (♦), and 0.012 (▲). The intensity increases with ϕ at all q. (b) $\phi = 0.16$ (●), 0.24 (◢), 0.30 (■), 0.39 (♦), 0.46 (▲), 0.53 (▼), and 0.57 (□). As ϕ increases, the intensity decreases at low q and a peak develops.

q. We obtain smooth results for all $S(q,\phi)$ up to q values in the vicinity of the interdroplet separation, and a clear peak in $S(q,\phi)$ is observed over a wide range of ϕ. At larger q, the calculated $S(q,\phi)$ becomes noisy due to the limited counting statistics, so the range of q is restricted to show the behavior of the primary peak. We observe a systematic decrease in the low-q value of S as ϕ is increased. Moreover, as ϕ is increased, we find that the observed peak in $S(q,\phi)$ goes through a maximum and the peak position moves to higher q.

To better demonstrate the rise and subsequent fall in the low-q intensity as ϕ is raised, we plot the intensity at the lowest measured q, I_L, as a function of droplet volume fraction in Fig. 4. As ϕ increases, a linear rise in $I_L(\phi)$ from $\phi = 0$ is followed by a peak and a subsequent drop. The linear

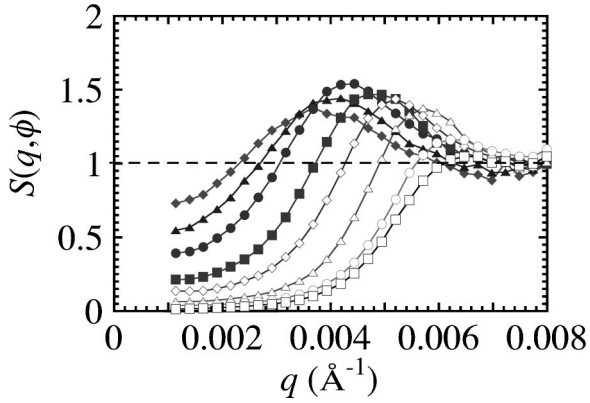

FIG. 3. Structure factor $S(q)$ of semidilute and concentrated nanoemulsions for a series of droplet volume fractions, $\phi = 0.079$ (♦), 0.012 (▲), 0.16 (●), 0.24 (■), 0.30 (◇), 0.39 (△), 0.46 (○), and 0.53 (□). Lines guide the eye. As ϕ increases, the depression at low q grows, and a peak appears at higher q; the position of the peak moves toward higher q, and the height of the peak exhibits a maximum.

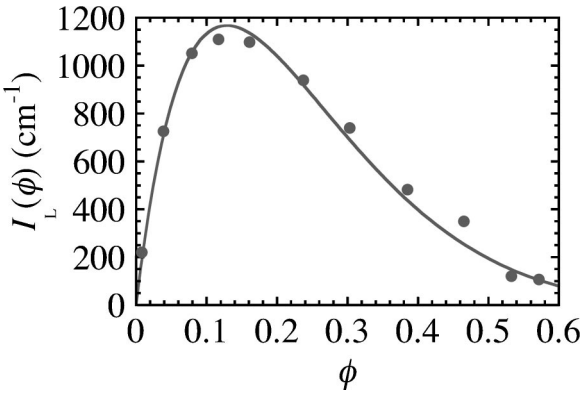

FIG. 4. Low-q intensity I_L of scattering measured for nanoemulsions as a function of droplet volume fraction ϕ. The solid line is the prediction for disordered hard spheres using the Percus–Yevick closure relation.

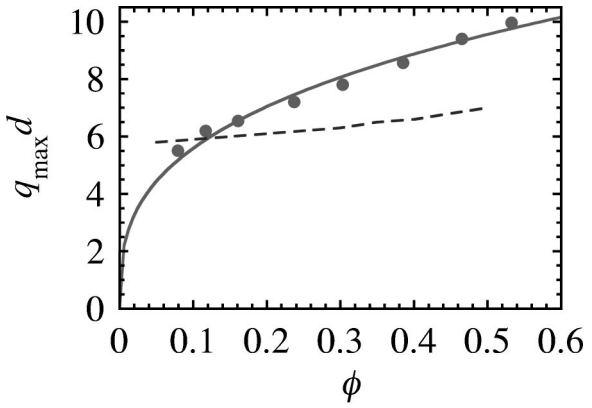

FIG. 6. Dimensionless wave number $q_{max}d$ associated with the first peak in the structure factor as a function of droplet volume fraction ϕ. The solid line is a fit to $q_{max}(\phi)d \sim \phi^{1/3}$ (see text). The dashed line is the PY prediction for hard spheres.

rise can be associated with the increase in the number density of droplets that scatter, and the drop is due to the increase in spatial correlation of the separations as droplets repel their neighbors nearby. For comparison, as we have previously done with concentrated asphaltene solutions,[30] we fit the emulsion data for $I_L(\phi)$ to $I_L^{HS}(\phi)=I_{rel}\phi S^{HS}(q,\phi)$, where $S^{HS}(q,\phi)$ is the Percus–Yevick (PY) structure factor for uniform hard spheres[8,31,32] (solid line). The only adjustable parameter in the fit is the relative intensity scale I_{rel} so the behavior of $I_L(\phi)$ for emulsions is well described by simple hard sphere theory.

We also plot the ϕ dependence of the value and position of the peak in $S(q,\phi)$. The behavior of the maximum value of the peak $S_{max}(\phi)$ is shown in Fig. 5, and the behavior of the q value associated with this peak $q_{max}(\phi)d$, where the average diameter $d=2a$, is shown in Fig. 6. We find a maximum in $S_{max}(\phi)$, and a continuous increase in $q_{max}(\phi)d$. The predictions for disordered uniform hard spheres using the PY closure relation are shown in both figures by the dashed lines. The qualitative behavior of the primary peak in $S(q,\phi)$ for nanoemulsions is different from PY hard sphere predictions. For example, PY hard spheres exhibit a strongly increasing S_{max} as ϕ increases toward the jamming point, whereas the nanoemulsion S_{max} goes through a maximum and even begins to decrease toward larger ϕ. Although the values of $q_{max}d$ for both PY hard spheres and nanoemulsions are close at low ϕ, they depart considerably at higher ϕ, and the nanoemulsion shows a peak that moves out to much higher q than the PY prediction.

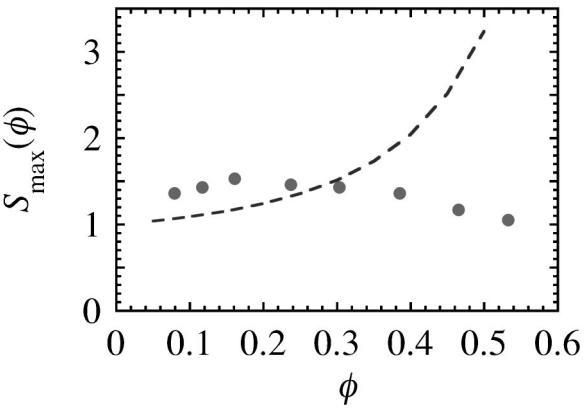

FIG. 5. Maximum value of the first peak in the structure factor, S_{max}, as a function of droplet volume fraction ϕ. The dashed line is the PY prediction for hard spheres.

Because the nanoemulsions investigated in this study interact through screened charge repulsions arising from the anionic stabilization by SDS, some aspects of the behavior of their structure with ϕ can resemble that of charged particulates, rather than hard spheres. For example, the position of the peak in $I(q,\phi)$ for slightly charged silica colloids has been observed to move significantly toward higher q for larger ϕ,[33] rather than changing very little as a function of ϕ, as is the case with hard spheres. Thus, such charged particulate systems exhibit an increase in $q_{max}(\phi)d$ that is much greater than what is predicted for PY hard spheres. Similarly, a more rapid increase in $q_{max}(\phi)d$ for charged droplets can arise because the repulsion can cause the droplets to become more strongly correlated (spatially) at lower volume fractions than would be expected for hard spheres. Depending upon the strength and range of the screened repulsion, the particles will form a configuration that tends to maximize the separation. In the extreme case of a strong repulsion with a large Debye screening length, the particles will even form colloidal crystals.[34] However, in our case, the repulsion between the nanodroplets is not this extreme, and no long-range translational order forms, so the positions of the centers of the nanodroplets are disordered. Nevertheless, the average separation between the repulsive droplets scales as $\phi^{-1/3}$, leading to a peak in the scattering at $q_{max}(\phi) \sim \phi^{1/3}$. A fit of $q_{max}(\phi)d=C\phi^{1/3}$ is shown in Fig. 6 (solid line), where $C=12.0\pm0.1$. Overall, the fit is in good agreement with the measurements, and the small deviations at the lowest ϕ can be attributed to the limited range of the repulsion whereas at the highest ϕ, the disorder and deformation of the droplets.

V. DISCUSSION

The complete behavior of $I(q,\phi)$ that we have observed could potentially be explained by a theory that accounts for the screened charge repulsion between the surfactant-coated interfaces of the deformable droplets, the disordered glassy structure, and the inherent polydispersity in the size of the

droplets. In rheological experiments performed on concentrated emulsions, we have found that the Debye repulsion could be taken into account by considering an effective volume fraction, $\phi_{\text{eff}}=\phi(1+\lambda_D/a)^3$, which includes a thin shell having thickness of the Debye length λ_D. In our case, $\lambda_D=3$ nm. Given the small size of the droplets, even this small screening length can significantly affect the effective droplet volume fraction. At the largest $\phi=0.57$, the effective volume fraction is actually $\phi_{\text{eff}}=0.64$. This implies that the droplets are only weakly deformed, yet they are concentrated enough to exhibit an elasticity and structure characteristic of a colloidal glass. For values of ϕ above those associated with the jamming point, the droplets must deform to some degree, yet we still divide using the form factor for spherical droplets. For these volume fractions, we are essentially showing an empirical "effective" structure factor, since we cannot deduce the form factor of the deformed droplets at high ϕ.

We have considered if the effects we observe could be attributed to the polydispersity of the droplets. Frenkel *et al.* have examined the structure factor of polydisperse hard spheres that have a log-normal distribution at two discrete volume fractions:[35] $\phi=0.3$ and $\phi=0.5$. In this work, they clearly show that increasing the polydispersity suppresses the primary peak in $S(q)$ at both volume fractions. This is similar to the lower values of $S_{\max}$ that we observe compared to monodisperse PY hard spheres. However, for polydispersities similar to those measured for our nanoemulsions, the maximum value of the peak is higher for $\phi=0.5$ than for $\phi=0.3$. This is not consistent with the trend of a decreasing $S_{\max}$ for increasing ϕ that we find for the most concentrated nanoemulsions. Therefore, it is unlikely that polydispersity can account for the observed trends for the structure of concentrated nanoemulsions. A complete theory of the structure of emulsion glasses that includes the screened charge repulsion and the deformability of the droplets could potentially account for ϕ dependence of the peak features that we have observed. Certainly, we have demonstrated that PY hard sphere theory explains the observed behavior of $I(q,\phi)$ at low q. At higher q, a simple scaling argument for repulsively charged droplets explains the observed q dependence of the peak, $q_{\max}(\phi)\sim\phi^{1/3}$, but the reduction in the magnitude of the intensity of the peak $S_{\max}(\phi)$ as ϕ approaches the jamming limit has not been observed for deformable objects, at least to our knowledge.

VI. CONCLUSION

In summary the observed behavior of the peak in the scattering from nanoemulsions is most likely due to the softness of the screened Coulomb interactions between the surfaces of the deformable liquid droplets that have a disordered glassy structure. A significant correlation between the positions of neighboring droplets begins to develop at values of ϕ larger than those associated with the peak in $I_L(\phi)$. However, the growth of long-range correlation is suppressed, and $S_{\max}(\phi)$ does not increase at larger ϕ as the disordered droplets begin to strongly interact with their neighbors and deform. The combination of the screened Coulomb repulsion and droplet deformation permits the droplet centers to approach more closely than impenetrable hard spheres and thereby enables $q_{\max}(\phi)d$ at large ϕ to significantly exceed the values found for Percus–Yevick hard spheres. A scaling argument based on repulsively interacting disordered colloids largely explains the trend in $q_{\max}(\phi)d\sim\phi^{1/3}$ that we have observed.

It would be interesting to understand the effective bulk properties, such as the structure factor, of random monodisperse foams that have been studied in simulations.[24] In order to compare with our data, the simulations would need to consider not only froths but also very wet foams that have a considerable polydispersity in droplet radius, which is known to affect the crystallization and jamming points for hard spheres.[36–38] Moreover, it would be useful to incorporate the screened Debye repulsion between the droplet interfaces. Once the three-dimensional structures of these foams have been created and appropriate scattering length densities have been ascribed to the dispersed and continuous phases, a Monte Carlo scattering simulation could provide the scattering intensity $I(q,\phi)$. It is likely that making all of these modifications to the existing simulations would be quite challenging.

Experimentally, it would be interesting to examine the structure of nanoemulsions that have been size fractionated to a greater degree, so that significant minima in the form factor are evident. In addition to reducing the size polydispersity, it would be useful to determine how changing the Debye screening length systematically alters the structure of the nanoemulsions. Raising the droplet volume fraction closer to the limit for a dry foam or froth could potentially reveal the average contributions of thin films, ridges, and plateau borders to the measured scattering intensity.

ACKNOWLEDGMENTS

The authors thank NIST's Center for Neutron Research for the beam time to perform these experiments, and they thank D. Frenkel, S. Milner, H. Reiss, and R. Bruinsma for useful discussions. They also thank J. McTague for supporting this work through the McTague Career Development Chair at UCLA.

[1] D. Myers, *Surfaces, Interfaces, and Colloids*, 2nd ed. (Wiley, New York, 1999).
[2] H. Reiss, J. Colloid Interface Sci. **53**, 61 (1975).
[3] J. Bibette, F. Leal-Calderon, and P. Poulin, Rep. Prog. Phys. **62**, 969 (1999).
[4] J. Ugelstad, F. K. Hansen, and S. Lange, Makromol. Chem. **175**, 507 (1974).
[5] P. L. Tang, E. D. Sudol, C. A. Silebi, and M. S. El-Aasser, J. Appl. Polym. Sci. **43**, 1059 (1991).
[6] K. Landfester, F. Tiarks, H. Hentze, and M. Antonietti, Macromol. Chem. Phys. **201**, 1 (2000).
[7] P. Taylor, Adv. Colloid Interface Sci. **106**, 261 (2003).
[8] J.-P. Hansen and I. R. McDonald, *Theory of Simple Liquids*, 2nd ed. (Academic, London, 1990).
[9] C. S. O'Hern, S. A. Langer, A. J. Liu, and S. R. Nagel, Phys. Rev. Lett. **86**, 111 (2001).
[10] C. S. O'Hern, S. A. Langer, A. J. Liu, and S. R. Nagel, Phys. Rev. Lett. **88**, 075507 (2002).
[11] T. G. Mason, M.-D. Lacasse, G. S. Grest, D. Levine, J. Bibette, and D. A. Weitz, Phys. Rev. E **56**, 3150 (1997).
[12] T. Tlusty and S. A. Safran, J. Phys.: Condens. Matter **12**, A253 (2000).
[13] W. B. Russel, D. A. Saville, and W. R. Schowalter, *Colloidal Dispersions*

(Cambridge University Press, Cambridge, 1989).
[14]P. N. Pusey and W. van Megen, Nature (London) **320**, 340 (1986).
[15]W. van Megen and S. M. Underwood, Phys. Rev. E **49**, 4206 (1994).
[16]B. J. Maranzano and N. J. Wagner, J. Rheol. **45**, 1205 (2001).
[17]E. R. Weeks and D. A. Weitz, Phys. Rev. Lett. **89**, 095704 (2002).
[18]S. Torquato, T. M. Truskett, and P. G. Debenedetti, Phys. Rev. Lett. **84**, 2064 (2000).
[19]A. Donev, I. Cisse, D. Sachs, E. A. Variano, F. H. Stillinger, R. Connelly, S. Torquato, and P. M. Chaikin, Science **303**, 990 (2003).
[20]D. J. Durian, D. A. Weitz, and D. J. Pine, Science **252**, 686 (1991).
[21]T. G. Mason, A. H. Krall, H. Gang, J. Bibette, and D. A. Weitz, in *Encyclopedia of Emulsion Technology*, edited by P. Becher (Marcel Dekker, New York, 1996), Vol. 4, p. 299.
[22]H. Gang, A. H. Krall, H. Z. Cummins, and D. A. Weitz, Phys. Rev. E **59**, 715 (1999).
[23]P. Hébraud, F. Lequeux, J. P. Munch, and D. J. Pine, Phys. Rev. Lett. **78**, 4657 (1997).
[24]A. M. Kraynik, D. A. Reinelt, and F. van Swol, Phys. Rev. E **67**, 031403 (2003).
[25]D. Weaire, S. Hutzler, S. Cox, N. Kern, M. D. Alonso, and W. Drenckham, J. Phys.: Condens. Matter **15**, S65 (2003).
[26]H. A. Stone, S. A. Koehler, S. Hilgenfeldt, and M. Durand, J. Phys.: Condens. Matter **15**, S283 (2003).
[27]K. Meleson, S. Graves, and T. G. Mason, Soft Materials (accepted).
[28]J. Bibette, D. Roux, and F. Nallet, Phys. Rev. Lett. **65**, 2470 (1990).
[29]M. Ungarish, Int. J. Multiphase Flow **21**, 267 (1995).
[30]T. G. Mason and M. Y. Lin, Phys. Rev. E **67**, 050401(R) (2003).
[31]R. J. Baxter, Aust. J. Phys. **21**, 563 (1968).
[32]N. W. Ashcroft and J. Lekner, Phys. Rev. **145**, 83 (1966).
[33]B. J. Maranzano, N. J. Wagner, G. Fritz, and O. Glatter, Langmuir **16**, 10556 (2000).
[34]E. B. Sirota, H. D. Ou-Yang, S. K. Sinha, P. M. Chaikin, J. D. Axe, and Y. Fujii, Phys. Rev. Lett. **62**, 1524 (1989).
[35]D. Frenkel, R. J. Vos, C. G. de Kruif, and A. Vrij, J. Chem. Phys. **84**, 4625 (1986).
[36]P. N. Pusey, J. Phys. (France) **48**, 709 (1987).
[37]S.-E. Phan, W. B. Russel, J. Zhu, and P. M. Chaikin, J. Chem. Phys. **108**, 9789 (1998).
[38]P. Bartlett, J. Phys.: Condens. Matter **12**, A275 (2000).